Microstructure Evolution and Online Thermal Resistance of Ag Sintered SiC/DBA Power Module During Power Cycling

Fupeng Huo [1], Ye Wang [2], Chuantong Chen [1], Zheng Zhang [1], Yoshiji Yamaguchi [3], Naoki Wakasugi [3], Aiji Suetake [1], Katsuaki Suganuma [1]
1 Flexible 3D System integration Laboratory, The Institute of Science and Industrial Research, Osaka University, Osaka, 567-0047, Japan
2 School of Reliability and Systems Engineering, Beihang University, Beijing, China
3 Yamato Scientific Co. Ltd., Tokyo, Japan
TEL: +81-06-6879-4294; FAX: +81-06-6879-8488
Email address: huofp@sanken.osaka-u.ac.jp

Abstract
With the increasing power and miniaturization of power electronics, the power cycling reliability and thermal management of power modules have become increasingly crucial. To address this issue, Our Lab. has developed a novel instrument that allows simultaneous power cycling and real-time thermal resistance measurement. Utilizing this specific instrument, we investigated the microstructural evolution of the die attachment layer during power cycling and monitored the real-time thermal resistance of the SiC-TEG (Silicon Carbide-Thermal Engineering Group) heater chip/sintered Ag/DBA (Directed Bonded Aluminum with the ceramic core of Si_3N_4) structure. Additionally, strategies to improve the degradation of the microstructure were proposed. The results indicate that after 10000 power cycles, numerous cracks were observed in the sintered Ag layer. However, the addition of 5 wt.% Al suppressed the generation of cracks significantly. The addition of Al particles has little effect on the transient thermal resistance during power cycling.

Key words
Power cycling, TEG chip, sintered Ag, DBA substrate, real-time thermal resistance

I. Introduction

Wide bandgap has attracted widespread attentions due to its excellent performance [1]. With the trends of high power and miniaturization of power module, the operating temperature has already reached to 200℃ [2]. This exceeds the service temperature of most lead-free solders. Therefore, sintered Ag technology is proposed, which was regarded as one of the promising approaches for the WBG die attach in power modules [3].

Thermal degradation of sintered Ag is a major factor affecting the reliability of power modules. Among these reliability tests, the power cycling test is used to simulate the junction temperature fluctuation process of the actual application of the device. This is achieved by passing the external load current on and off. It is considered the most important experiment for evaluating the reliability of power module packaging [4,5]. On the other hand, with the increasing thermal generation resulting in higher power, effective thermal management is becoming more and more important, especially for real-time monitoring and measurement of the thermal characteristics of power modules.

Unfortunately, until now, there is no one equipment that can perform power cycle experiments and simultaneously conduct real-time measurement of transient thermal resistance of power module. To solve this issue, our laboratory has developed a device that can simultaneously perform power cycling and real-time measurement of thermal resistance [6]. Based with the specific instrument, the microstructure evolution and real-time thermal characteristics of SiC heater chip/sintered Ag/DBA structure under different power cycles were investigated by X-ray micro-computed tomography (μ-CT) and scanning electron microscopy (SEM). In addition, the strategies to improve power cycle reliability of SiC TEG-heater chip /sintered Ag/DBA power modules are also proposed.

II. Experimental procedure

A. Sample fabrication

The structure of the TEG-chip is shown in Fig. 1(a). Its dimensions are 5 mm × 5 mm × 0.35 mm. The chip is composed of four main parts: Pt heater, Pt sensor, heater's electrode, and sensor's electrode. Additionally, the electrode surfaces were sputtered with Au and on the backside of the chip, a Ti adhesive layer and a Ag metal layer were sputtered. The schematic of the DBA substrate is depicted in Fig. 1(b). Micro-scale Ag flakes (Fukuda Metal Foil and Powder Ltd, Kyoto, Japan) were mixed with the organic solvent CELTOL-IA (Daicel Corporation, Japan) to prepare the Ag paste. Similarly, Ag-5Al (by mass fraction) composite paste was prepared using a similar method. The paste was then printed on the DBC substrate, and the TEG-chip was mounted on the paste as shown in Fig. 1(b). Subsequently, the samples were heated to 250°C on a hotplate in air and kept at this temperature for 60 minutes without applying pressure. Afterward, they were cooled to room temperature.

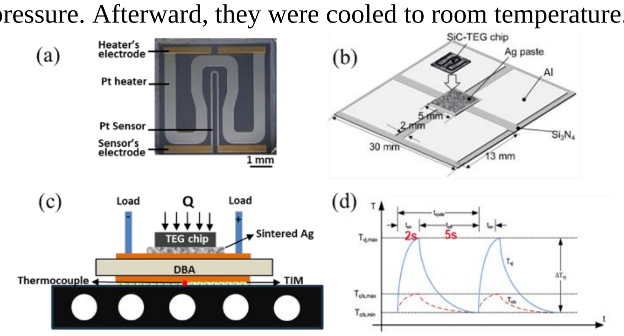

Fig. 1 Schematic of instrument system. (a) TEG heater chip, (b) DBA substrate, (c) sample mounting platform, (d) power cycling profile.

B. Real-time thermal resistance-power cycle test platform

The sample mounting platform is illustrated in Figure 1(c), which is connected to a power source and control system. The samples were installed on the cooling plate (maintained at a constant 25℃) through a Thermal Interface Material (TIM). In this system, the heat generated by the TEG chip is transferred to the cooling plate via the die attach materials and DBA substrate. The temperature gradient can be readily obtained. Based on the temperature difference (ΔT) between the surface of the heater chip and the bottom of the DBA substrate, the thermal resistance (Rth) can be calculated using the following formulas (1) and (2).

$$Rth=\Delta T/Q \quad (1)$$

$$\Delta T=T_{\text{surface of SiC}}-T_{\text{bottom of DBA}} \quad (2)$$

Where, Q is the joule heat generated by TEG- chip, ΔT is the temperature difference.

The power cycling profile is depicted in Fig. 1(d). The power supply was turned on for 2 seconds, reaching a junction temperature of 200℃, and then turned off for 5 seconds, allowing the junction temperature to drop to room temperature. During the power cycling process, real-time thermal resistance was recorded. Cracks and microstructure evolution in the die attachment layer were studied using X-ray micro-computed tomography (μ-CT) and scanning electron microscopy (SEM).

III. Results and Discussion

The X-μ CT images of sintered Ag/DBA and sintered Ag-5Al/DBA joints are shown in Fig. 2. Fig. 2(a) displays the X-μ CT image of Ag/DBA joint at the initial stage. It can be observed that no cracks or defects are evident, indicating a good bonding between the sintered Ag and DBA substrate. In Fig. 2(b), the X-μ CT image of the Ag/DBA joint after 10000 power cycles reveals various cracks. The sintered Ag layer shows a significant degradation after 10000 power cycles. This degradation behavior is attributed to the differences in coefficient of thermal expansion (CTE) among the materials in the joints. Fig. 2(c) displays the X-μ CT image of the sintered Ag-5Al/DBA joint at the initial stage, similar to Fig. 2(a), no cracks are observed. After 10000 power cycles, cracks are observed in the Ag-5Al sintered layer, but the crack density is significantly lower than that of the sintered Ag. This indicates that the addition of Al particles effectively inhibits crack formation.

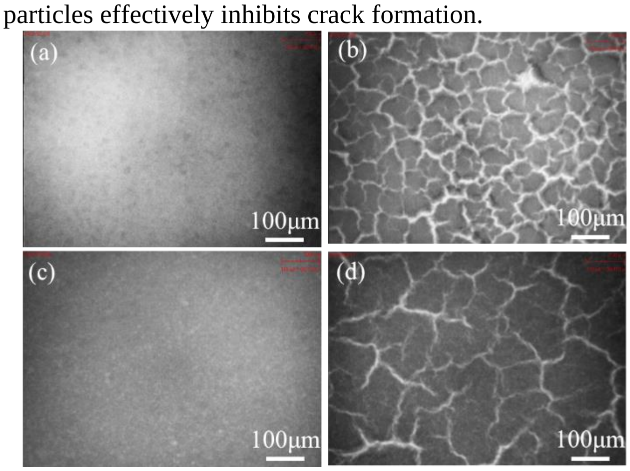

Fig.2 X-μ CT images of sintered Ag/DBA at (a) initial stage, (b) 10000 cycles. sintered Ag-5Al/DBA at (c) initial stage, (d) 10000 cycles.

To further investigate the microstructural evolution of the die attachment layer during power cycling, their microstructure was observed. Fig. 3 displays the SEM images of the sintered Ag/DBA and Ag-5Al/DBA joints before and after power cycling. Fig. 3(a) shows the SEM image of the sintered Ag/DBA joint at the initial stage, composed of three parts: the upper part of TEG-chip, the lower part of DBA substrate, and sandwiched between them of the sintered Ag layer. The sintered Ag exhibits a uniform porous structure and well bonded with both the TEG-chip and DBA substrate, demonstrating the excellent sintering performance of micro-scale Ag flakes. Fig. 3(b) presents the microstructure of the Ag/DBA joint after 10000 power cycles. The DBA substrate undergoes severe plastic deformation during the power cycling process. This is attributed to the low yield strength of Al itself and high frequency temperature changes. As for the sintered Ag layer, the microstructure transforms from a uniform continuous sintered Ag layer to a coarser and fractured one. Many longitudinal cracks can be observed. The coarsening of the microstructure is attributed to the thermal effects during the power cycling process. The generation of numerous cracks is due to the alternating loads applied during power cycling [7], causing the sintered Ag layer to continuously endure tensile and compressive stresses at the interface. Additionally, unlike bulk Ag, sintered Ag exhibits poor ductility, which is also a concern for its application [8]. Therefore, under the continuous action of alternating loads, many cracks are generated. Regarding the TEG-chip, due to the inherent hardness of SiC, it is difficult for it to undergo deformation. Under the influence of alternating loads, stress accumulates continuously, eventually resulting in delamination at the interface between the sintered Ag and the chip.

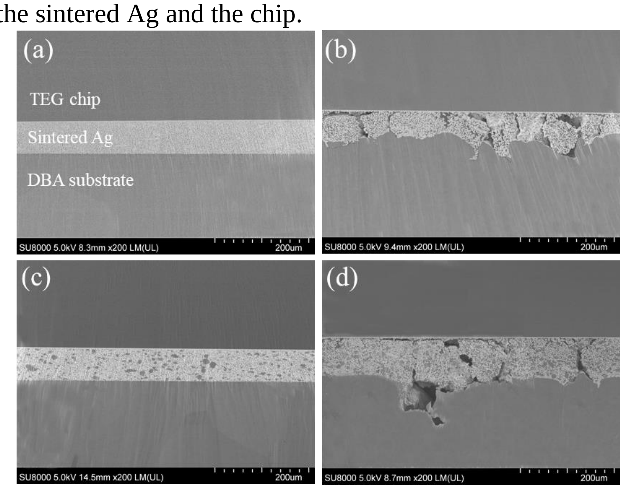

Fig. 3 SEM images of the sintered Ag/DBA joint at (a) initial stage, (b) 10000 cycles. sintered Ag-5Al/DBA at (c) initial stage, (d) 10000 cycles.

Fig. 3(c) shows the SEM image of the sintered Ag-5Al/DBA joint after bonding. The DBA substrate and chip appears flat, and in the die attachment layer, Al particles are uniformly distributed within the Ag matrix, indicating a successful preparation of the Ag-5Al composite paste. Moreover, the sintered Ag-5Al layer exhibits good bonding with both the TEG-chip and DBA substrate. After 10000 power cycles (Fig. 3(d)), the microstructure of the Ag-5Al/DBA joint undergoes some degradation. However, the overall degree of degradation is notably weaker than that of pure Ag/DBA joint (as shown in Fig. 3(b)). For the DBA substrate, plastic deformation occurs after 10000 power cycles, but the extent of deformation is milder than that in Fig. 3(b). As for the sintered Ag-5Al layer, the density of cracks is also lower than that in Fig. 3(b). Thus, the degradation of the joint is effectively suppressed with the addition of Al particles. This can be attributed to the effective reduction of CTE mismatch between the die attachment layer and the DBA substrate after the addition of Al particles, thereby lowering the stress in the joint and inhibiting crack formation.

From Fig. 2 and 3, we can observe that the addition of Al effectively suppresses crack formation. Additionally, there is an interesting phenomenon worth noting, which is the direct bonding between sintered Ag and Al substrate. As is well known, connecting to Al is challenging due to the naturally formed Al2O3 thin film on the surface of Al, which has been widely documented [9,10], especially in low-temperature connections in the field of electronic packaging. However, in this study, it is achieved through low-temperature and pressure-less sintering. Fig. 4 shows the interface between sintered Ag and the DBA substrate. Fig. 4(a) displays the interface between sintered Ag and the DBA substrate after bonding, revealing a good bonding between sintered Ag and the substrate. The magnified image of area 1 in Fig. 4(a) is shown in Fig. 4(b), it demonstrates a tight bonding between the Ag sintered neck and Al, with no observable gaps in the bonding region. Fig. 4(c) shows the SEM image of the interface after 10000 power cycles. The DBA substrate undergoes severe deformation, yet there is still an effective connection between the substrate and the sintered Ag, except for the fractured region of the sintered Ag. The magnified image of area 2 in Fig. 4(c) (shown in Fig. 4(d)) illustrates that the Ag sintered neck remains tightly bonded to Al despite undergoing severe deformation. These results indicate that using micro-scale Ag flakes enables effective bonding between sintered Ag and the DBA substrate, and the Ag/Al bonding interface exhibits good power cycling reliability. The direct bonding between sintered Ag and Al reduces the usage of a metallization layer, lowering the overall thermal resistance and cost of the entire power module, making it highly promising for industrial applications.

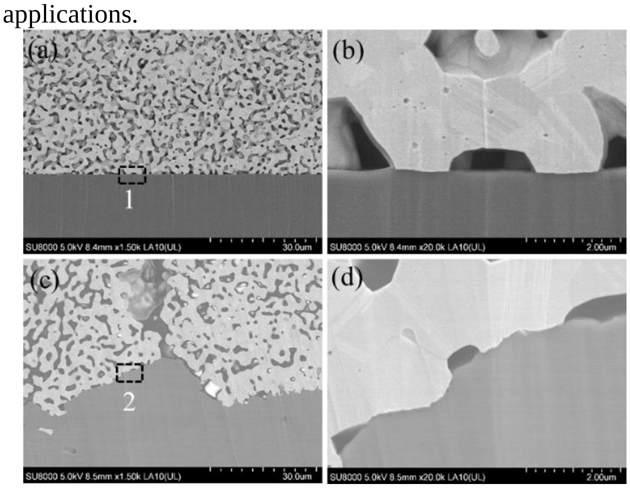

Fig. 4 Interface between sintered Ag and the DBA substrate at (a) initial stage and (c)10000 cycles. (b) Magnified image of area 1. (d) Magnified image of area 2.

Not only sintered Ag /DBA but also Ag-5Al/DBA joints can achieve effective bonding, and similar phenomena can be observed, so it will not be elaborated further here.

Additionally, the connection between sintered Ag matrix and Al particles in Ag-5Al sintered layer has also caught our attention. Fig. 5 illustrates the interface between sintered Ag and Al particles in the Ag-5Al sintered layer. Fig. 5(a) shows the microstructure of the sintered Ag-5Al, with Al particles uniformly distributed within the Ag matrix. The magnified image of area 1 in Fig. 5(a) (shown in Fig. 5(b)) demonstrates that the Ag sintered neck tightly attaches to the surface of Al particles, indicating effective bonding. Furthermore, in the surface region of Al particles (marked with a dotted circle), some nanoscale clusters can be observed, which is one of the reasons why micro-scale Ag flakes can directly bond with Al. During the Ag flake sintering process, Ag nanoparticles ejection phenomenon occurs [11], and these Ag nanoparticles possess extremely high surface energy. Acting as bridges, these Ag nanoparticles facilitate the bonding between sintered Ag and Al. Fig. 5(c) shows the microstructure of Ag-5Al after 10000 power cycles, and from the observation of crack paths, it can be inferred that fractures occur both within the sintered Ag and at the Ag/Al interface. There is no significant tendency for fractures to occur at the Ag/Al interface, indicating that the strength of the Ag/Al particle bonding is comparable to the strength of the sintered Ag. This implies that the addition of Al does not compromise the mechanical strength of the die attachment material after power cycling. Fig. 5(d) is the magnified image of area 2 in Fig. 5(c), revealing that, despite experiencing severe plastic deformation, the sintered Ag remains firmly bonded to the Al particles. In conclusion, under the conditions of low-temperature, pressure-less, and air atmosphere, micro-scale Ag flakes can form effective bonding with Al, exhibiting good power cycling reliability.

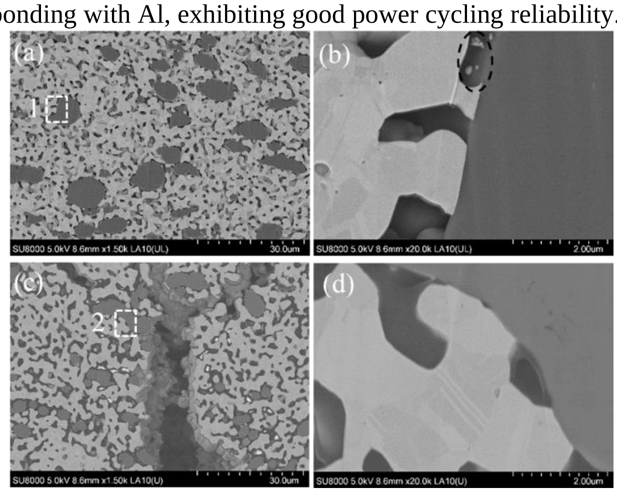

Fig. 5 Interface between sintered Ag and Al particles in the Ag-5Al sintered layer at (a) initial stage and (c)10000 cycles. (b) Magnified image of area 1. (d) Magnified image of area 2.

Thermal resistance is an important parameter for assessing the heat dissipation capability of power modules [12]. Fig. 6 shows the real-time thermal resistance of the power module during power cycling. For the TEG chip/sintered Ag/DBA structure, the initial transient thermal resistance is 0.903 K/W. And after 10000 power cycles, it reaches 0.910 K/W. This indicates that the power module with sintered Ag demonstrates excellent heat dissipation stability. As for the TEG-chip/sintered Ag-5Al/DBA structure, the initial transient thermal resistance is 0.907 K/W, almost the same as the sintered Ag. After 10000 power cycles, the transient thermal resistance increases to 0.937 K/W, representing only a 3.4% growth compared to the initial stage. This result shows that the power module with sintered Ag-5Al also exhibits good heat dissipation performance during power cycling. Moreover, as mentioned above, the addition of Al particles effectively suppresses crack formation. Therefore, Ag-5Al is considered a promising die attachment material for application in power modules.

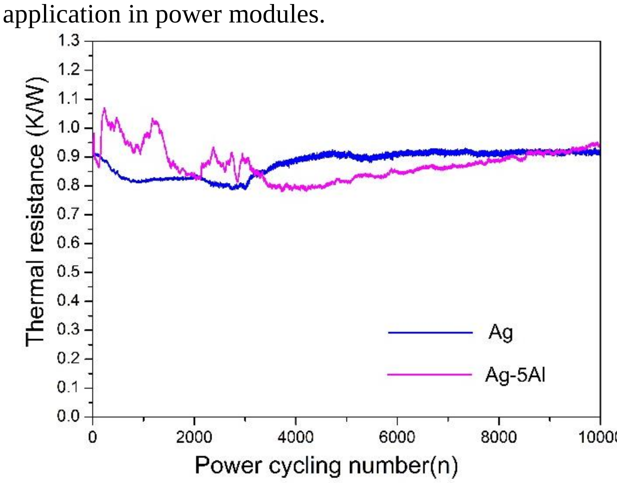

Fig. 6 the real-time thermal resistance of the power module during power cycling.

IV. Conclusion

Sintered Ag flakes exhibit excellent bonding with the DBA substrate, which can be attributed to the injection of Ag nanoparticles during sintering. As the power cycle number increases, the microstructure of the sintered Ag layer coarsens, and the occurrence of cracks gradually increases. This phenomenon is mainly attributed to the severe plastic deformation of the DBA substrate during power cycling, as well as the mismatch in CTE between sintered Ag and Al in the DBA substrate. To suppress the generation of cracks, an Ag-5Al paste was introduced. The results show that the cracks in the Ag-5%Al composite paste are substantially reduced compared to those in the Ag paste under the same power cycling period. This reduction can be attributed to the moderated CTE difference between sintered Ag and DBA achieved by the addition of Al. The power module with sintered Ag demonstrates excellent heat dissipation stability. The addition of Al particles has little effect on the transient thermal resistance during power cycling, and after 10,000 cycles, the thermal resistance was 0.937 K/W, only increased by 3.4%, also exhibiting good heat dissipation performance during power cycling. Therefore, Ag-5Al is considered a promising die attachment material for application in power modules.

Acknowledgment

This work was supported by a project (JPNP20004) commissioned by the New Energy and Industrial Technology Development Organization (NEDO) and JSPS KAKENHI Grant Number JP22K04243, and by a research grant from The Murata Science Foundation.

References

[1] Z. Zhang, C. Chen, A. Suetake, M. C. Hsieh, and K. Suganuma, "Reliability of Ag Sinter-Joining Die Attach Under Harsh Thermal Cycling and Power Cycling Tests," J. Electron. Mater., vol. 50, no. 12, pp. 6597–6606, 2021.

[2] C. Chen et al., "Interface-Mechanical and Thermal Characteristics of Ag Sinter Joining on Bare DBA Substrate during Aging, Thermal Shock and 1200 W/cm2Power Cycling Tests," IEEE Trans. Power Electron., vol. 37, no. 6, pp. 6647–6659, 2022.

[3] Z. Zhang, C. Chen, A. Suetake, M. C. Hsieh, A. Iwaki, and K. Suganuma, "Pressureless and low-temperature sinter-joining on bare Si, SiC and GaN by a Ag flake paste," Scr. Mater., vol. 198, p. 113833, 2021.

[4] P. D. Reigosa, H. Luo, and F. Iannuzzo, "Implications of ageing through power cycling on the short-circuit robustness of 1.2-kV SiC mosfets," IEEE Trans. Power Electron., vol. 34, no. 11, pp. 11182–11190, 2019.

[5] L. R. GopiReddy, L. M. Tolbert, and B. Ozpineci, "Power cycle testing of power switches: A literature survey," IEEE Trans. Power Electron., vol. 30, no. 5, pp. 2465–2473, 2015.

[6] D. Kim et al., "Online Thermal Resistance and Reliability Characteristic Monitoring of Power Modules with Ag Sinter Joining and Pb, Pb-Free Solders during Power Cycling Test by SiC TEG Chip," IEEE Trans. Power Electron., vol. 36, no. 5, pp. 4977–4990, 2021.

[7] D. Wilson and F. P. E. Dunne, "A mechanistic modelling methodology for microstructure-sensitive fatigue crack growth," J. Mech. Phys. Solids, vol. 124, pp. 827–848, 2019.

[8] Y. Liu et al., "Plasticity enhancement of nano-Ag sintered joint based on metal foam," J. Mater. Sci. Mater. Electron., vol. 32, no. 6, pp. 7187–7197, 2021.

[9] X. Wu, Y. Li, C. Ma, P. Jiang, and J. Sun, "Study on phase evolution of the resin bonded Al-Al2O3 composites in N2-flowing at high temperature," J. Alloys Compd., vol. 784, pp. 1145–1152, 2019.

[10] H. Xue, X. Wei, W. Guo, and X. Zhang, "Bonding mechanism study of active Ti element and α-Al2O3 by using first-principle calculation," J. Alloys Compd., vol. 820, p. 153070, 2020.

[11] S. K. Lin et al., "Nano-volcanic eruption of silver," Sci. Rep., vol. 6, pp. 1–9, 2016.

[12] S. Rashidi, H. Shamsabadi, J. A. Esfahani, and S. Harmand, A review on potentials of coupling PCM storage modules to heat pipes and heat pumps, vol. 140, no. 4. Springer International Publishing, 2020.